Bakar, M.A; Alam, Farhan; Das, Moumita,; Barg, Sobhi; Bertilsson, Kent "Reconfigurable three state dc-dc power converter for the wide output range applications," *IECON 2019 - 45th Annual Conference of the IEEE Industrial Electronics Society*, pp.4911-4916, 14-17 October 2019
10.1109/IECON.2019.8927652

Reconfigurable three state dc-dc power converter for the wide output range applications

M.Abu Bakar, Farhan Alam, Moumita Das, Sobhi Barg, Kent Bertilsson
Department of Electronic Design, Mid Sweden University, SWEDEN
ORCID iD: 0000-0002-7802-0795

***Abstract*—Improving the dc voltage gain of power converters has been the primary focus of the current and past research in the area of power electronics. This work presents another solution to widen the range of the output voltage. It proposes three reconfigurable steps for the output voltage. The range of the output voltage varies up to four times the base level. These configurations together vary the output voltage from 15 to 96 volts. A soft switched dc-dc power converter is built with the traditional topology of phase shifted full bridge converter along with improved characteristics. For better management of the transformer loss, a configuration of four transformers has been employed. The proportional gate drive approach is implemented to obtain four similar isolated blocks of the output voltage. This makes it possible to either configure these blocks all in series, parallel or in series/ parallel combination of two. The concept is verified in a low-profile prototype. The hardware is characterized up to the load power of 1kW for the input voltage of 400Vdc. The converter reports better efficiency over the complete range of output voltage.**

Keywords—wide output, isolated output converter, reconfigurable converter, ZVS converter, series transformers, proportional gate drive

I. Introduction

There is a growing trend in the industry to put all solutions in a single box. To meet this requirement, the power unit is required to be isolated, having a wide range of dc conversion ratio. On the other hand, the power unit should meet the need for high reliability, high power density and high efficiency [1]. For example, in electric vehicles, fuel cell vehicles and renewable energy sources, there is a growing demand for compact, intelligent and efficient wide output dc-dc isolated power converters. The converter should achieve line and load regulation for the complete range of operation. The traditional solution to obtain a wide range of output voltage is the bench type variable output power supplies [2]. These solutions could be linear power supplies or switch mode power supplies. None of the solution meet the present requirement because of being bulky and less efficient. Furthermore, these solutions have limitations in the steps to make a wide change in the output voltage.

Power converters are generally designed for a nominal working condition. Converters show desired performance while working within those conditions. Although some power converters propose optimum performance in a wide range of the input voltage, however, the output voltage of the converters remains constant. In applications where supercapacitors are used as an energy storage device, it would be advantageous if the output voltage of the converter is adjusted over a wide range as the capacitor is being charged. In order to meet the requirement of a wide range of the output voltage, multiple power converters are usually stacked together. This increases the cost and complexity of the system [3]. Moreover, it degrades the redundancy and efficiency of the overall system. Many research efforts [1], [2], [4]–[9] have been reported to widen the range of the output voltage. Most of the works are based on the variable frequency LLC power converters. Apart from various advantages, LLC converters have few limitations. The zero current switching in rectifiers is lost as the switching frequency crosses above the resonance frequency, it makes it hard to keep the output voltage constant [9]. The variable frequency operation further adds the complexity regarding EMI. In [7], secondary side phase shifted control is proposed to extend the range of the output voltage, however, the addition of buck, balance and boost modes makes the control complex.

This work presents a unique one-box solution to widen the range of the output voltage as well as keeping the efficiency of the converter stable. This dc-dc converter is combined with three reconfigurable states to get the desired output voltage for the intended application. For example, in case of high current applications, it configures the output voltage to X volt, for medium current applications, it configures the output voltage to 2X ǁ 2X volt. For the applications where there is a demand for high voltage and less current, it configures the output voltage to 4X volt. By using these configurations, the output voltage of the

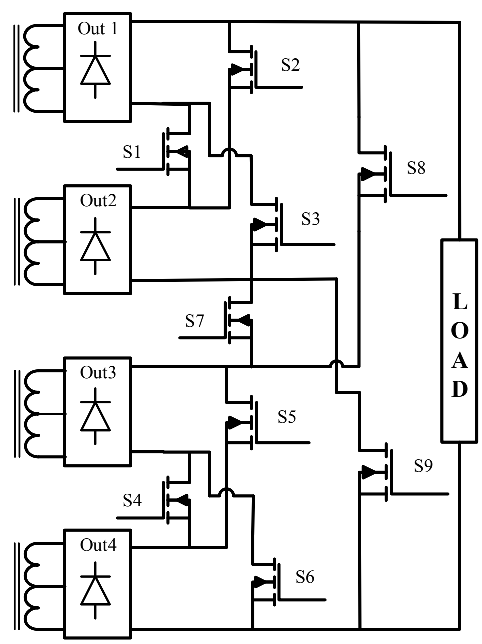

Fig. 1. Block diagram of the output section of the proposed converter.

proposed converter can be adjusted from 15V to 96V. All of the configurations provide electrical isolation between the line voltage and the output voltage. The simplified block diagram of the output section of the proposed converter is shown in Fig. 1.

The main part of the converter is based on the topology of phase shifted full bridge converter. A configuration of four transformers has been implemented in the proposed converter. This provides four separate output blocks. These blocks are isolated not only from the line voltage but also from each other. This resembles these blocks as four batteries, which can be configured either as parallel or series. The main contributions of this work are outlined as follows:-

1. Since the proposed converter provides three reconfigurable steps for the wide range of output voltage, it could be the best candidate among space-constrained applications.
2. Instead of a single bulky transformer, the proposed converter is built with four series transformers. It helps to reduce the weight and volume of the converter. The total transformer loss spreads among four transformers, which simplifies heat management.
3. For high current applications, the converter configures all the four outputs in parallel, which equally share the total load current. This reduces the stress on the secondary rectifiers by a factor of four.
4. This work provides the simple to implement a solution to the industry by presenting a dc-dc solution along with the well-documented phase shifted full bridge topology.

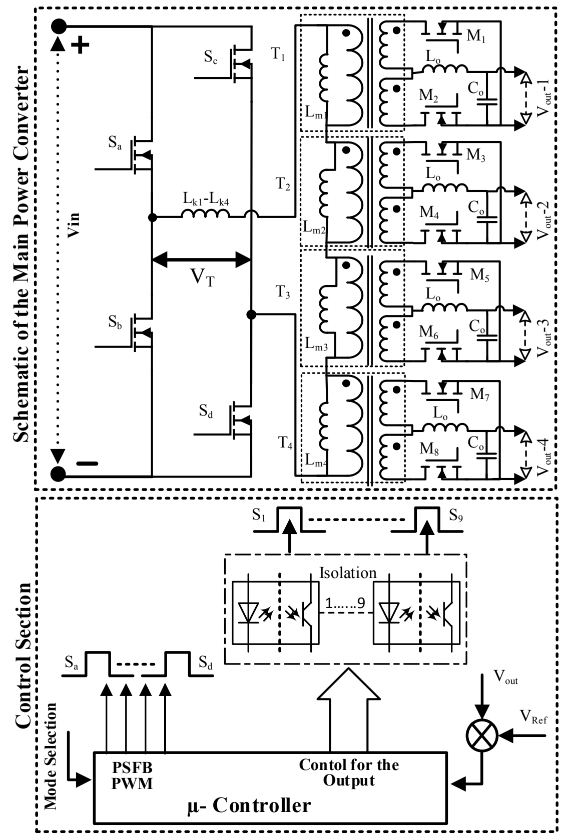

Fig. 2. Circuit diagram of the main converter.

II. Circuit Configuration

The primary configuration of the proposed converter is a phase shifted full bridge converter as shown in Fig. 2. The power devices S_a-S_d makes the two legs of the converter. Here the devices S_a-S_b and S_c-S_d are respectively configured as the leading leg and the lagging leg of the converter. A combination of four center-tapped transformers T_1-T_4 replaces the main transformer of the conventional phase shifted full bridge converter. The primary windings are connected in series. The series connection on the primary side ensures the flow of an equal amount of current through all four transformers. Similarly, when all output sections are configured in parallel, the secondary windings equally share the load current [10]. The inductors L_{M1}-L_{M4} represent the magnetizing inductance of each transformer. The inductor L_{k1}-L_{k4} represents the combined intrinsic leakage inductance of transformers T_1-T_4. The devices M_1-M_8 are the synchronous rectifiers, connected with the center-tapped secondary windings of the transformers. The rectified voltage of each winding is then filtered through separate inductor L_o and capacitor C_o.

The output stage Fig. 1, of the converter, consists of three main sections. The devices S_1-S_9 are the main switches to configure the output voltage. These sections together make the arrangement to configure the output voltage in any of the three possible states. In order to prevent any short-circuit among these switches, electrical isolation has been implemented. For this, the switching of these switches is kept in line by using the optically isolated gate drivers. Likewise, the power supplies for the drivers are also carried out in a way to ensure isolation for the proper operation. The switching of the whole system is controlled by using a single digital signal processor. The control section is divided into two parts. One part controls the switching of the main phase shifted full bridge converter, and the other part controls the output devices S_1-S_9. The output section can remotely be configured for the desired output voltage. This can be configured either by implementing the provision of USB connectivity or by using the latch switches.

III. Working Principle of the Converter

The electronics of the proposed converter is a combination of two separate sections. First section steps down the input dc voltage to four isolated blocks of the output voltage having the same level of the voltage. The second section configures these output voltage sources in series or in either parallel or in series-parallel. It means the working of both sections differs from each other. Therefore, the working of each part will be explained one by one.

A. Main Section of the Converter

The main dc-dc power converter works on the principle of a conventional phase shifted full bridge converter. The primary difference is the power transformer. In this converter, a configuration of four planar transformers replaces the single main transformer. The working of the phase shifted full bridge converter has been extensively discussed in the literature and is being referred to previous work [11]. Therefore, in order to keep this summary short, the discussion is limited to the proposed set of components.

The configuration of four series transformers on the primary side acts as a potential divider. This divides the input to the transformers by a factor of four i.e. $V_{in}/4$. The input voltage on the primary side can be written as

$$V_{in} = V_T \;= V_{t1} + V_{t2} + V_{t3} + V_{t4}$$

where V_{in} is the line voltage and V_{t1}- V_{t4} are the voltage across the primary winding of transformers T_1 - T_4 . The loss in transformer cores is determined by the applied volt-second. Since in this configuration the applied volt-second is reduced by a factor of four, this spreads the total core loss among four transformers. This distribution of the total loss results in less heat dissipation, consequently the less heat management efforts. The magnetizing inductance and resonance inductance can be written as

$$L_M = L_{m1} + L_{m2} + L_{m3} + L_{m4}$$

$$L_K = L_{k1} + L_{k2} + L_{k3} + L_{k4}$$

where L_M and L_K are respectively the total magnetizing inductance and the leakage inductance. L_{m1}-L_{m4} and L_{k1}-L_{k4} are the individual magnetizing inductance and the leakage inductance of transformers T_1-T_4. The magnetizing inductance L_M, is the combined inductance, which decreases the amount of the current that circulates through the primary windings during the freewheeling period. Similarly, the total leakage inductance L_K, acts as a resonance inductance to achieve zero voltage switching of the primary devices, it eliminates the need of an extra bulky inductor.

In phase shifted full bridge converter, the energy stored in the leakage inductor along with the output capacitance of the same leg devices resonates to obtain the zero voltage switching. In that case, the combined leakage inductor L_K, takes part to reach the zero voltage switching. When either of the diagonal device pair S_a, S_d or S_b, S_c starts conducting, the power is delivered from the primary section to the secondary section. The synchronous devices M_1-M_8 rectify the secondary winding voltage. The dc voltage conversion ratio of the converter is

$$V_{out} \;= 2D\,\frac{N_s}{N_p}\left(\frac{V_{in}}{4}\right)$$

where V_{out} is the output voltage, D is the effective duty ratio of a single transformer, N_p and N_s are respectively the number of primary and secondary turns. In order to extend the range of the output voltage, here each output block needs to be isolated from each other. To accomplish this, the synchronous rectifiers of each block should also be isolated. An approach of proportional gate drive synchronous rectification is adopted for this purpose. This approach not only eliminates the need of external gate driver for the synchronous devices but also minimizes the conduction time for the body-diodes [12]. This improves the efficiency and reduces the component count. The circuit diagram of one of the block of synchronous reification is shown in Fig. 3. The drain-node of two synchronous devices M_1-M_2 are connected with the secondary windings of the center-tapped transformer. The common end of the transformer is connected with the filtering components, inductor L_o, and capacitor C_o. The voltage after rectification passes through the filtering components to get a smooth output voltage.

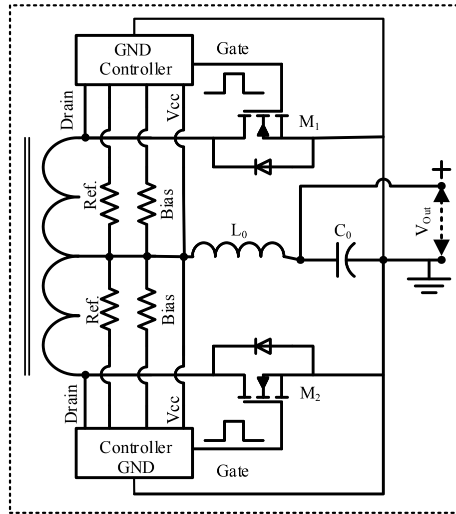

Fig. 3. A section of the synchronous rectification.

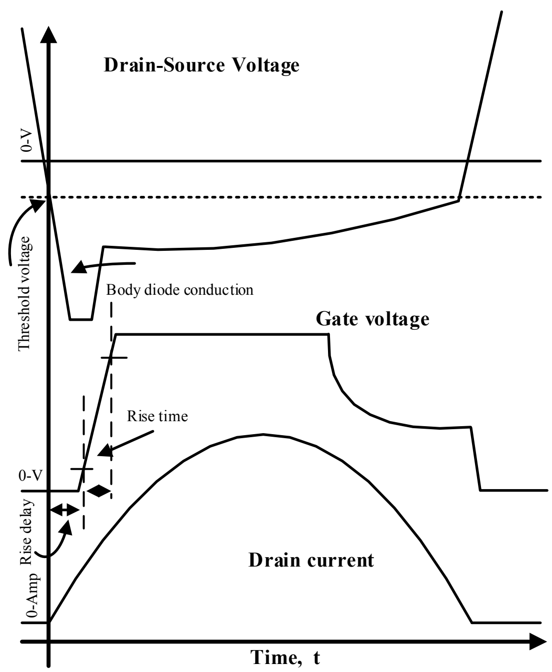

Fig. 4. Working principle of the proportional gate drive.

The generated dc voltage provides the necessary power and biasing to the respective controller. This makes each block of the synchronous rectification completely isolated from each other. It also simplifies the synchronous rectification by eliminating the necessity of external command signals. As shown in Fig. 4, [12] the drain sense terminal of the controller constantly monitors the drain-source voltage of the synchronous device. As the voltage on the secondary winding goes negative, the body diode of the device becomes forward biased. The moment drain voltage reaches the threshold voltage, a positive voltage is applied on the gate of the synchronous device. The controller starts sourcing the current and turns ON the device. The applied voltage on the gate becomes proportional to the drain-source voltage of the device. This keeps the device turn

ON for the majority of the cycle and minimizes the conduction loss due to the body diode. When drain current decays, the drain-source voltage also decays, this in turn, decreases the applied gate-source voltage to turn OFF the synchronous device.

B. *Working of the Output Section*

The output part of the converter contains three main sections. There are nine MOSFET switches in these sections. The orientation of each switch is selected so that the body diodes do not interfere. It means that the body diode remains reverse biased as long as the switch is idle. Furthermore, in order to ensure the isolation of every MOSFET, the ON/OFF switching is controlled by the addition of optical isolators in the control path. Similarly, the power supplies for these isolated drivers are also arranged in a way to ensure the required functionality. The status of every switch is very significant to accomplish the desired goal. This is acquired by incorporating with the digital signal processor. The status of the switch is configured according to the required level of the output voltage. If it is required to connect all the output blocks in series, then switches $S_1, S_4,$ and S_7 turn ON while keeping all other switches OFF. The logic states given in Table 1, show the status of each switch for all possible levels of the output voltage. As seen in the table, all sections together make the arrangement to configure the output blocks in order to achieve the desired level of the output voltage.

TABLE 1. GATE STATUS OF THE SWITCHES

Mode	**Switch Status**								
	S_1	S_2	S_3	S_4	S_5	S_6	S_7	S_8	S_9
All Series	1	0	0	1	0	0	1	0	0
All parallel	0	1	1	0	1	1	0	1	1
Seies/ parallel	1	0	0	1	0	0	0	1	1

As stated earlier, the proposed converter can switch between three output voltage states. The dc voltage conversion ratio of the converter is also different in each state. In case, all the blocks of the output voltage are configured in parallel, the dc voltage gain of the converter can be determined as

$$V_{out} \ = \frac{1}{2} D \frac{N_S}{N_p} (V_{in}) \qquad (1)$$

V_{out} is the voltage that appears on the output terminals of the converter. N_s/N_p is the transformer turn ratio of each block of the output stage, which is equal for all the four transformers. In a case, when all the outputs are required to configure in series, this increases the output voltage by a factor of four. In such a case, the dc conversion ratio becomes

$$V_{out} \ = 2D \frac{N_S}{N_p} (V_{in}) \qquad (2)$$

Similarly, for the third configuration (series and parallel) of the output voltage, the output block-1 makes a series connection with the block-2, and block-3 makes the series connection with block 4. These two series-connected blocks are then connected in parallel, i.e.

$$V_{out} \ = (V_{out1} + V_{out2}) \parallel (V_{out3} + V_{out4})$$

where V_{out1}-V_{out4} , represent the individual voltage of each block. The dc conversion ratio for this configuration is given as

$$V_{out} \ = D \frac{N_S}{N_p} (V_{in}) \qquad (3)$$

IV. EXPERIMENTAL INVESTIGATIONS

In order to verify the proposed converter, a prototype is designed on the printed circuit board (PCB). The value of the key components required to design a phase shifted full bridge converter, e.g., peak current, effective duty ratio, flux density, resonance inductance, voltage/current stress, has been calculated using the guideline is given in [13]–[15]. The main converter and all the output stages are built on the same PCB. The control part is built on a separate PCB. Plugin type connectors are assembled to connect both PCBs. The whole electronics is made compact by choosing the low profile passive and active components. Planar transformer structure is adapted to further minimize the volume and weight of the finished converter. The proportional gate drive for the synchronous devices is implemented by using the part number ZXGD3105. Part number TLP701 provides the optical isolation to the switches of the three state output sections.

The converter is characterized for all the three proposed configurations to achieve a wide range of the output voltage. In order to make the demonstration understandable, first the input/output voltage of the main converter has been set to a certain level, then the desired output voltage to the load is configured in the output control section. Each configuration of the output voltage is investigated for the variation in load power. The specification of the converter along with the information about the key components is given in Table 2.

The transformer core utilized in this design example is the PQ series due to its low profile and high-efficiency characteristics. Both primary and secondary windings are constructed by using PCB traces. In order to enhance the current carrying capacity of the PCB traces, the parallel winding structure has been adapted. The key parameters of the transformer are given in Table 3. The magnetizing/leakage inductance and ac resistance of the winding are measured by using Bode-100 impedance analyzer.

TABLE 2. SPECIFICATIONS AND THE COMPONENT DETAIL OF THE CONVERTER

Input voltage (V_{in})	400 V_{dc}
Output voltage (V_o)	15-96 V_{dc}
Output power (P_o)	1 kW
Frequency (*f*)	200 kHz
Duty cycle (D_{max})	0.48
Device, S_a-S_d	GS66508B
Synchronous devices, M_1-M_8	320N20NS
Switches S_1-S_{11}	SI872ADB
Capacitor *(Co)*	68µF
Output inductor (L_o)	1µH
µ Controller (DSP)	dSJ33f504

TABLE 3. KEY PARAMETERS OF A SINGLE TRANSFORMER

Core material	Magnetics Inc P-material
Core shape/size	PQ 20/20
Core material	3C95
Primary/secondary winding mutual inductance, L_p/L_s	190/12 µH
Primary/secondary leakage inductance, L_{kp}/ L_{ks}	1.3/0.1 µH
Primary/secondary winding ac resistance, R_p/R_s	120/20 mΩ
Primary to secondary turn ratio, N_p/N_s	4:1:1

In order to verify the effective turn ratio of the transformers, the differential voltage V_T on the series-connected primary winding of all the transformers, along with the output voltage of the converter is captured. For this, the voltage on the common point of both legs is measured by using the differential probe, and the output voltage is monitored on the output terminal of the converter. Fig. 5 shows the differential voltage on the primary winding of the transformers and the output voltage. In the figure, channel one shows the bridge voltage on the primary winding of the transformer, which approximately equals the line voltage $V_T = \pm 400V_{dc}$. Since this is the input to the series combination of four transformers, the stress on each transformer is $V_t = 400/4$, this reduces the volt-second stress on the transformer by a factor of four. Here the transformer turns ratio is 4:1:1, using eq. (1), the base output voltage of the converter should be $V_{out} = 24V_{dc}$. Channel four in Fig. 5 shows the level of the output voltage, which comes out approximately 24V_{dc}.

The switching of the output voltage from one state to the other is captured by using the trigger function available in the oscilloscope. Fig. 6 shows one of the waveforms when the output voltage switches between two states. It can be seen in the figure, the initial level of the voltage is 24V, it means all the blocks of the output voltage are configured in parallel and when it configures all blocks in series, the output voltage jumps to 24x4=96V.

As discussed, the proportional gate drive approach is implemented in this work, which reduces the conduction time of the body diode in synchronous rectification. This is analyzed by simultaneously capturing both the primary bridge voltage and the drain node voltage of the synchronous device. Fig. 7 shows the bridge voltage and drain-source voltage of one of the synchronous device. As seen, the body diode conducts for a very short time, the device starts conducting as the bridge voltage reaches the input voltage V_{in} , in either direction.

The soft switching in the lagging leg of the phase shifted full bridge converter has been a tedious task to achieve for the complete range of working conditions. This leg loses zero voltage switching for the light load conditions. To enhance this range, an external inductor is usually connected in series with the main transformer. Since this work uses four series-connected transformers, the combined leakage inductance makes it possible to achieve the ZVS of the lagging leg over a wide range of the load. The soft switching characteristics of this prototype is observed on the oscilloscope. Since it is simple to capture the signal with reference to the ground, the switching action of only the low side power devices of both the leading leg and the lagging leg have been observed. Fig. 8 shows that the device of

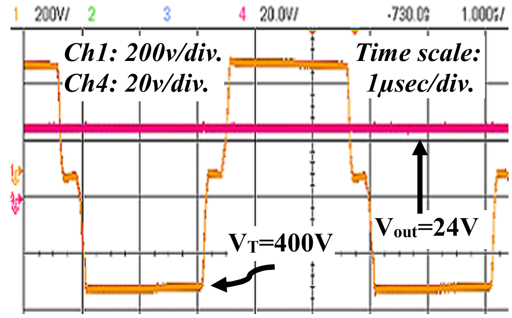

Fig. 5. dc voltage conversion, Ch-1 voltage on the primary winding of the transformers, Ch-4 output voltage of the converter.

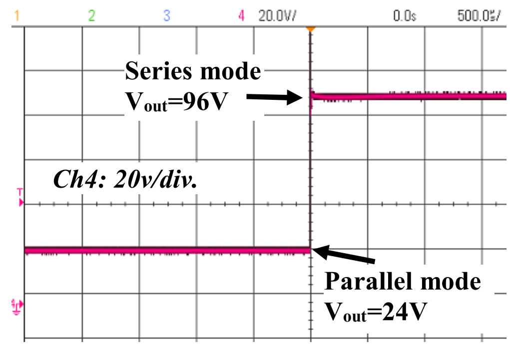

Fig. 6. Transition of the output voltage from one state to the other.

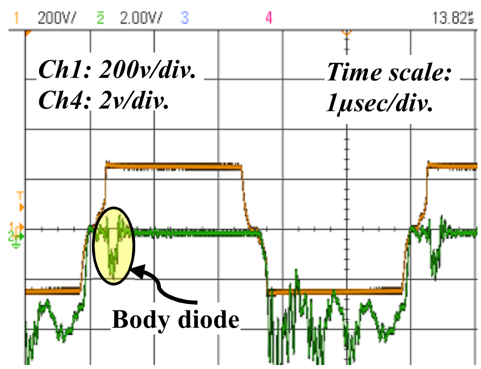

Fig. 7. Proportional gate drive, Ch-1 primary winding differential voltage, Ch-2 drain-source voltage of the synchronous device.

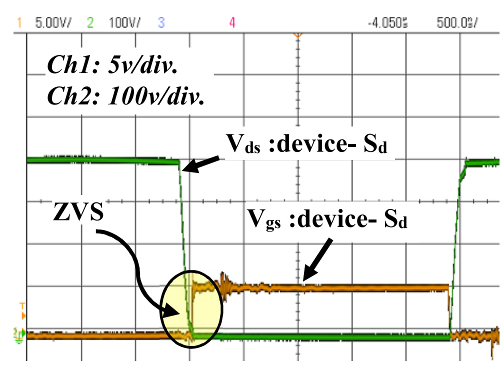

Fig. 8.ZVS of lagging leg at 5% of the rated load, Ch-1 gate-source voltage of the device S_d, Ch-2 drain-source voltage of S_d.

the lagging leg observe complete zero voltage switching at light load i.e. at 5% of the rated load.

In order to make comparison in the performance of the proposed configurations, the efficiency of the converter is also measured separately for all the three states as well as for the complete range of the output voltage. The efficiency is recorded by using the Zimmer LMG500 power analyzer. The performance of each configuration is evaluated for the same range of the load power. Fig. 9 shows this comparison. As seen, the comparison shows similar performance. In the case, V_{out} = 24V, efficiency slightly drops, this is due to the reason that, all the blocks of the output voltage are configured as parallel. In such a case the load current is about 70% higher as in the case V_{out} = 96V. It results in more conduction loss for this configuration. Fig. 10 shows the efficiency over the full range of the output voltage V_{out} = 15-96V for constant load. It is recorded by setting fist the base voltage, then three configurations are applied. The efficiency varies from 90% to 95%.

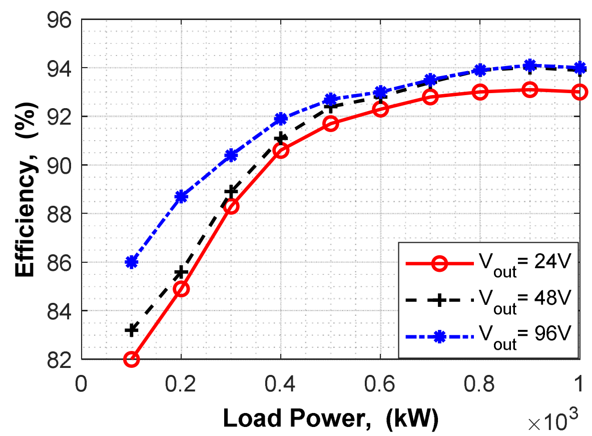

Fig. 9. Efficiency curves of the converter for each configuration.

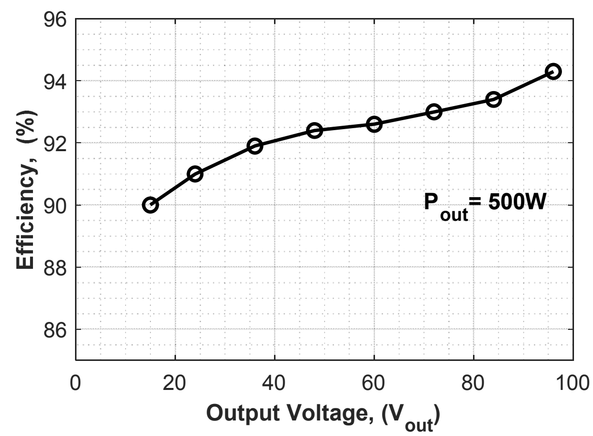

Fig. 10. Efficiecy of the converter for variations in the output voltage.

CONCLUSION

In this work, a three-state reconfigurable converter is presented for wide output applications such as regenerative braking system, where the wide variation of the output voltage is the main requirement. The converter can be configured from any base voltage X to 2X or 4X. It makes it possible to vary the output voltage for a wider range of 15V-96V. The proposed structure has been successfully demonstrated in the conventional soft switched phase shifted full bridge converter, which further makes it simple to implement. The configuration of small series transformers instead of using a single bulky transformer simplifies the heat management efforts and reduces the weight by 40% as compared to counterparts. The efficiency of the reported range of the output voltage varies from 90% to 95%. As a part of future work, the efficiency will further be improved by adopting the separate control strategy for each configuration.

REFERENCES

[1] M. Kim, H. Jeong, B. Han, and S. Choi, "New Parallel Loaded Resonant Converter With Wide Output Voltage Range," *IEEE Trans. Power Electron.*, vol. 33, no. 4, pp. 3106–3114, Apr. 2018.

[2] P. Sun, L. Zhou, and K. M. Smedley, "A reconfigurable structure DC-DC converter with wide output range and constant peak power," *IEEE Trans. Power Electron.*, vol. 26, no. 10, pp. 2925–2935, 2011.

[3] Bo Yang, Peng Xu, and F. C. Lee, "Range winding for wide input range front end DC/DC converter," in *APEC 2001. Sixteenth Annual IEEE Applied Power Electronics Conference and Exposition (Cat. No.01CH37181)*, 2002, vol. 1, pp. 476–479.

[4] E. S. Kim, J. Lee, Y. Heo, T. Marius, J. Ju, and Y. S. Kook, "LLC resonant converter with wide output voltage control characteristics according to operating mode transition," *Conf. Proc. - IEEE Appl. Power Electron. Conf. Expo. - APEC*, vol. 2018–March, pp. 2117–2123, 2018.

[5] M. Shang and H. Wang, "LLC converter with reconfigurable voltage multiplier rectifier for high voltage and wide output range applications," in *IECON 2017 - 43rd Annual Conference of the IEEE Industrial Electronics Society*, 2017, pp. 1279–1285.

[6] B. Axelrod, Y. Berkovich, and A. Ioinovici, "High Efficiency Parallel Post Regulator for," *Proc. 2003 Int. Symp. Circuits Syst. 2003. ISCAS '03.*, vol. 3, no. 2, pp. 852–858, 2003.

[7] H. Wu, L. Chen, and Y. Xing, "Secondary-Side Phase-Shift-Controlled Dual-Transformer-Based Asymmetrical Dual-Bridge Converter With Wide Voltage Gain," *IEEE Trans. Power Electron.*, vol. 30, no. 10, pp. 5381–5392, 2015.

[8] S. Cetin and A. Astepe, "A phase shifted full bridge converter design for electrical vehicle battery charge applications based on wide output voltage range," *Int. Conf. Appl. Electron.*, vol. 2016–Septe, pp. 51–56, 2016.

[9] H. Wu, X. Zhan, and Y. Xing, "Interleaved LLC Resonant Converter with Hybrid Rectifier and Variable-Frequency Plus Phase-Shift Control for Wide Output Voltage Range Applications," *IEEE Trans. Power Electron.*, vol. 32, no. 6, pp. 4246–4257, 2017.

[10] Y. Shen, W. Zhao, Z. Chen, and C. Cai, "Full-Bridge LLC Resonant Converter With Series-Parallel Connected Transformers for Electric Vehicle On-Board Charger," *IEEE Access*, vol. 6, pp. 13490–13500, 2018.

[11] M. A. Bakar, F. Alam, and K. Bertilsson, "A phase shifted full bridge converter with novel control over the leakage inductance," in *2016 18th European Conference on Power Electronics and Applications (EPE'16 ECCE Europe)*, 2016, vol. 19, no. 4, pp. 1–10.

[12] Diode Incorporated, "Datasheet, Synchronous MOSFET Controller ZXGD3105N8," 2015.[Online].Available: https://www.diodes.com/assets/Datasheets/ZXGD3105N8.pdf.

[13] R. W. Erickson and D. Maksimović, *Fundamentals of Power Electronics*, no. July. Boston, MA: Springer US, 2001.

[14] X. Ruan, *Soft-Switching PWM Full-Bridge Converters*. Singapore Pte. Ltd.: John Wiley & Sons, Ltd, 2014.

[15] Z. Chen, M. Li, and Y. Wang, "Wide-range ZVS phase-shifted full-bridge converter with low circulation loss," *IECON Proc. (Industrial Electron. Conf.*, pp. 1882–1888, 2014.